








Evaluation of Twenty-Flavonoid Derivatives as Possible Interleukin-6 Inhibitors Using a Theoretical Model

Figueroa-Valverde Lauro ^{1,*}, Díaz-Cedillo Francisco ², Rosas-Nexticapa Marcela ³, Alvarez-Ramirez Magdalena ³, López-Ramos Maria ^{1,*}, Mateu-Armand Virginia ³, Garcimarrero-Espino E. Alejandra ³

¹ Laboratory of Pharmaco-Chemistry, Faculty of Chemical Biological Sciences, University Autonomous of Campeche, Av. Agustín Melgar s/n, Col Buenavista C.P. 24039 Campeche, Camp., México

² School of Biological Sciences of the National Polytechnic Institute- Prol. Carpio y Plan de Ayala s/n Col. Santo Tomas, México, D.F. C.P. 11340

³ Faculty of Nutrition, University Veracruzana, Médicos y Odontólogos s/n C.P. 91010, Unidad del Bosque Xalapa Veracruz, México

* Correspondence: lfiguero@uacam.mx (F.L.); maclopez@uacam.mx (L.M.)

Scopus Author 55995915500

Received: 9.04.2023; Accepted: 24.06.2023; Published: 4.02.2024

Abstract: There are some studies that suggest that interleukin-6 can modulate cancer cell growth. It is important to mention that some drugs have been used to inhibit the biological activity produced by interleukin-6 on cancer cells. However, their interaction with this biomolecule is very confusing. Analyzing these data, the aim of the investigation was to carry out a theoretical study on the interaction of twenty-flavonoid derivatives with interleukin-6. Besides, 1N26 protein and interleukin-6 inhibitors such as madindoline A, clarithromycin, and tenidap were used as theoretical tools in the DockingServer program. The results showed different amino acid residues were involved in the interaction of flavonoid derivatives with 1N26 protein surface compared with madindoline A, clarithromycin, and tenidap. Other results show that the inhibition constant (K_i) for flavonoid derivatives such as 1, 2, 5, 10, 13, 18, and 19 was lower than that of madindoline A. Finally, the K_i for 11 was lower than for clarithromycin and tenidap. In conclusion, the flavonoid derivatives 1, 2, 5, 10, 11, 13, 18, and 19 could be a good alternative as interleukin-6 inhibitors to decrease cancer cell growth.

Keywords: cancer; interleukin-6; flavonoids; 1N26.

© 2024 by the authors. This article is an open-access article distributed under the terms and conditions of the Creative Commons Attribution (CC BY) license (<https://creativecommons.org/licenses/by/4.0/>).

1. Introduction

Cancer is one of the leading causes of death worldwide [1-4]; this pathology clinic is conditioned for several factors, such as genetics [5, 6], drugs [7, 8], dietary fatty acid pattern [9], and cigarette smoking [10]. It is important to mention that there are drugs to treat several types of cancer such as avelumab [11], dactinomycin [12], tamoxifen [13], atezolizumab [14], dutasteride [15], blinatumomab [16], doxorubicin [17] and others. However, some of these drugs can produce some secondary effects, such as neutropenia [18], cardiotoxicity [19], and ocular toxicity [20]. In the search for new therapeutic alternatives, some flavonoids have been used as therapeutic agents; this may be due to antioxidant [21-23], anti-inflammatory [24, 25], and anticancer effects [26, 27]. In this way, a study suggests that a flavonoid (silibinin) may exert anticancer activity against human ovarian cancer cells by increasing apoptosis and inhibiting the epithelial-mesenchymal transition [28]. Other data indicate quercetin may decrease nasopharyngeal carcinoma growth by regulating YAP (yes-associated protein) [29].

Recently, a study showed that another type of flavonoid, such as chrysin, could affect genomic stability in breast cancer cells by suppressing DNA double-strand break repair [30]. Furthermore, one report indicates that genistein inhibits human prostate cancer cell growth by regulating the caspase-3 pathway [31]. Other data show that lutein may inhibit tumor progression in lung cancer cells through the ATR/Chk1/p53 signaling pathway [32]. In addition, a study showed that naringenin decreases cancer cell growth through cyclin-dependent kinase 6 inhibition [33]. Other data showed that combined treatment of naringenin/epicatechin suppressed colon carcinoma cell survival and epithelial-mesenchymal transition (a phenomenon that leads to functional changes in cell migration and invasion) [34]. Another study displays that naringin inhibits tumor growth and reduces interleukin-6 and tumor necrosis factor- α levels in Rats with Walker 256 Carcinosarcoma (a mixed tumor with sarcomatous and parenchymal components) [35]. All these data indicate that flavonoids can act as carcinogenic agents through interaction with some biomolecules; however, their interaction with interleukin-6 is not very clear on cancer cell growth. Analyzing these data, this study aimed to assess the possibility that several flavonoids could interact with interleukin-6 using the 1N26 protein as a theoretical model. Besides, clarithromycin, benzoxazole derivative, madindoline-A, and tenidap anticancer drugs were used as controls on DockingServer software.

2. Material and Methods

2.1. Methodology general.

Figure 1 shows the chemical structure of twenty flavonoid derivatives (compounds 1 to 20), which were used as theoretical tools to assess their potential interaction with interleukin-6 as follows:

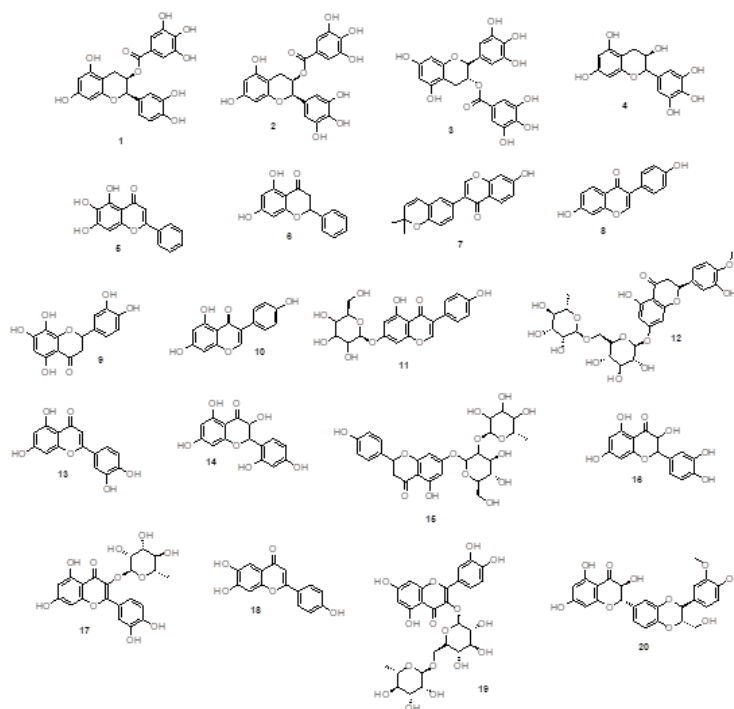


Figure 1. Structure chemical of flavonoid derivatives (1 to 20), **1.** (-)-Epicatechin gallate, **2.** (-)-Epigallocatechin gallate, **3.** (-)-Gallocatechin gallate, **4.**(-)-Gallocatechin, **5.** Baicalein, **6.** Chrysin, **7.** Corylin, **8.** Daidzein, **9.** Eriodictyol, **10.** Genistein, **11.** Genistin, **12.** Hesperidin, **13.** Luteolin, **14.** Morin, **15.** Naringin, **16.** Quercetin 2, **17.** Quercitrin, **18.** Rutin, **19.** Scutellarein, **20.** Silibinin

2.2. Physicochemical parameters.

Electronic parameters such as HOMO (Highest Occupied Molecular Orbital), LUMO (Lowest Unoccupied Molecular Orbital) energy, orbital coefficients distribution, molecular dipole moment, HBD (hydrogen bond donor groups), HBA (hydrogen bond acceptor groups) and PSA (polar surface area) were determined using the SPARTAN'06 software [36].

2.3. Ligand-protein.

The binding of flavonoid derivatives with Interleukin-6 was determined using 1N26 (PDB DOI: <https://doi.org/10.2210/pdb1N26/pdb>) [37] protein as a theoretical model. In addition, to evaluate the thermodynamic parameters involved in flavonoid derivative-protein complex formation, the DockingServer program was used [38].

2.4. Pharmacokinetic evaluation.

Theoretical pharmacokinetics involved in the chemical structure of flavonoid derivatives (1, 2, 5, 10, 11, 13, 18, and 19) were determined using the SwissADME software [39, 40].

2.5. Toxicology analysis.

Toxicity evaluation for flavonoid derivatives 1, 2, 5, 10, 11, 13, 18, and 19 was determined using GUSAR software [41].

3. Results and Discussion

There are some reports that interleukin-6 may be associated with increased growth of cancer cells [4-11]; for this reason, a theoretical study was conducted in this investigation to evaluate the possibility that flavonoid derivatives could interact with interleukin-6 surface using the DockingServer program.

3.1. Physicochemical parameters analysis.

There are several studies indicating that molecular orbitals (HOMO/LUMO) and their frontier electron density are theoretical tools to predict the reactivity of a molecule [42, 43]. For example, a report showed the frontier molecular orbitals (HOMO-LUMO gap) levels of some flavonoids such as catechin, quercetin, luteolin, and taxifolin using the density functional theory method [44]. Other studies show the frontier orbitals (HOMO/LUMO) of either catechin or epicatechin using Gaussian calculations to predict the reactivity of these compounds [45]. Analyzing these data in this study, HOMO, LUMO, and HOMO-LUMO gap for flavonoid derivatives (compound 1 to 20) were determined using the Spartan'06 software (Figures 2-5 and Table 1). The results showed that the HOMO-LUMO gap value for compound 7 (10.08 eV) was lower compared to flavonoid derivatives 1-6 and 8-20 (Table 1); this phenomenon could be conditioned by the molecular orbital that is located in the phenyl and other groups. All these data suggest that functional groups could induce changes in the organic superconductivity of flavonoid derivatives as happens; this phenomenon could bring consequence variations in the electronic transmittance.

Table 1. Theoretical evaluation of physicochemical parameters of flavonoid derivatives (1-20) using SPARTAN'06 software.

Compound	HOMO	LUMO	ΔE	PSA	LogP	μ	HBD	HBA
1	-8.53	2.16	10.69	158.13	2.46	4.74	7	9
2	-8.62	2.18	10.80	176.19	2.07	6.55	8	10
3	-8.29	2.21	10.50	175.71	2.07	5.70	8	10
4	-8.57	3.66	12.23	117.89	1.11	4.44	6	7
5	-8.54	1.71	10.25	71.30	1.40	3.73	3	5
6	-8.84	2.37	11.21	55.38	2.02	2.79	2	4
7	-7.72	2.36	10.08	46.47	3.15	4.60	1	4
8	-8.25	2.30	10.55	59.86	2.18	2.29	2	4
9	-8.34	2.12	10.46	109.34	0.85	6.83	5	7
10	-8.44	2.16	10.60	74.36	1.74	4.33	3	5
11	-8.51	2.03	10.54	140.56	-0.10	4.30	6	10
12	-8.11	2.80	10.91	193.05	-1.22	13.78	8	15
13	-8.66	1.81	10.47	92.67	1.01	3.30	4	6
14	-8.75	2.26	11.01	112.18	0.58	4.17	5	7
15	-8.89	2.07	10.96	188.19	-1.10	8.89	8	14
16	-8.51	2.05	10.56	112.20	0.58	1.65	5	7
17	-8.25	1.99	10.24	160.14	-1.21	7.02	7	11
18	-7.85	2.65	10.50	227.93	-2.96	11.08	10	16
19	-8.51	2.06	10.57	78.15	1.40	5.86	3	5
20	-8.55	1.98	10.53	131.91	1.53	2.17	5	10

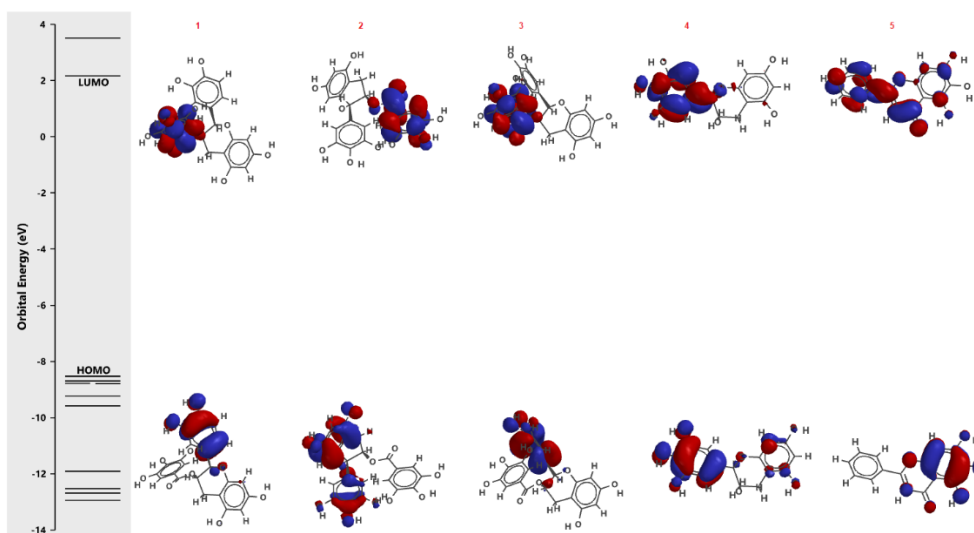


Figure 2. The scheme shows the molecular orbitals (HOMO and LUMO) involved in compounds 1 to 5, visualized with SPARTAN'06 software.

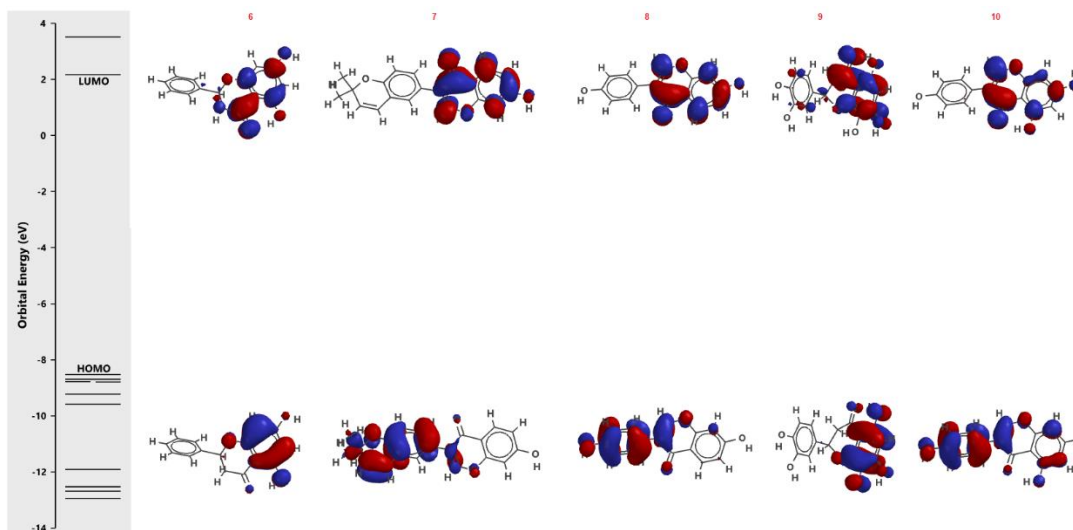


Figure 3. Frontiers orbitals (HOMO and LUMO) involved in compounds 6 to 10, visualized with SPARTAN'06 software.

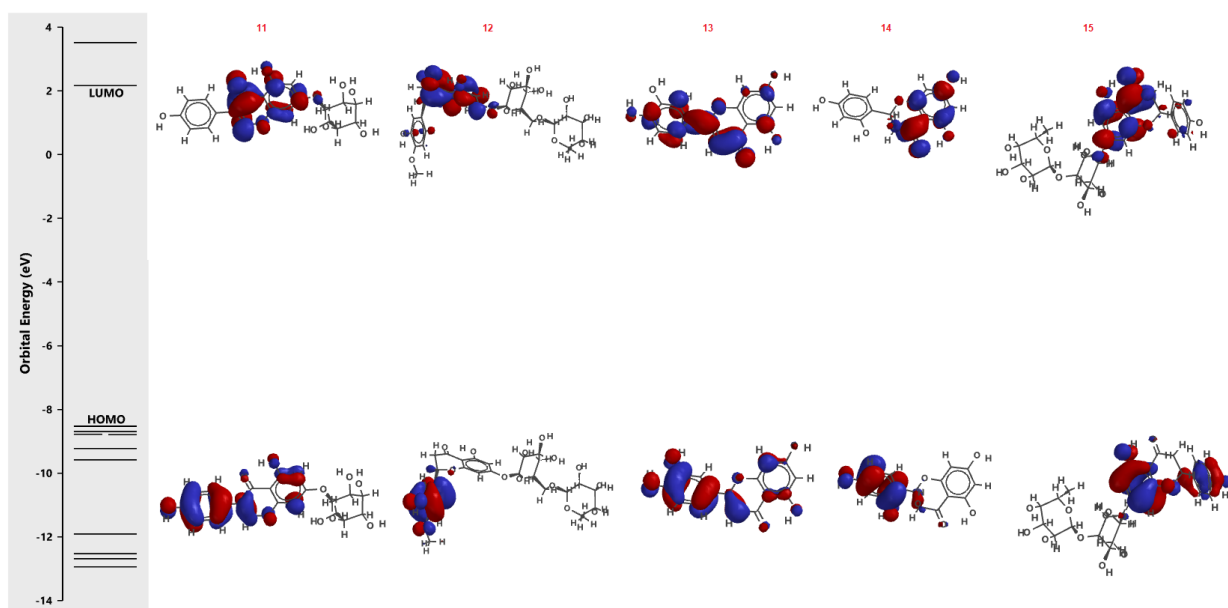


Figure 4. The scheme shows the frontier orbitals (HOMO and LUMO) involved in compounds 11 to 15, visualized with SPARTAN'06 software.

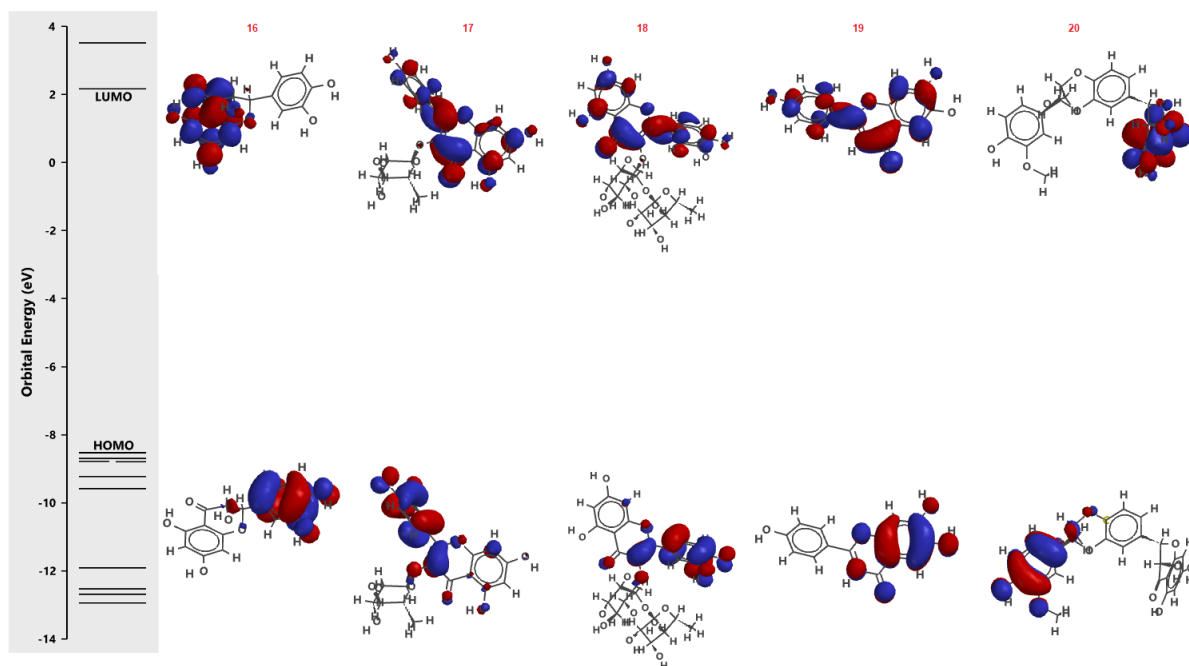


Figure 5. Frontiers orbitals (HOMO and LUMO) involved in the compounds 16 to 20, visualized with Spartan'06 software.

3.2. Interaction ligand-protein.

It is important to mention that some methods have been used to predict the interaction of several compounds with different biomolecules; for this reason, these methods have had wide applications in designing new compounds with biological activity. Analyzing this data, in this research, a theoretical evaluation was carried out to evaluate the interaction of flavonoid derivatives (compounds 1 to 20) with the Interleukin-6 surface using the 1N26 protein (Crystal Structure of the extracellular domains of human interleukin-6 receptor alpha chain) [37] as control. Besides, some interleukin-6 inhibitors, such as madindoline A [46], clarithromycin [47], and tenidap [48], were used as theoretical tools in DockingServer software. The results (Table 2) showed different amino acid residues involved in the interaction of flavonoid

derivatives (compounds 1 to 20) with 1N26 protein surface compared with madindoline A, clarithromycin, and tenidap; this phenomenon may be due to differences in their chemical structure (Figures 1 and 2).

Table 2. Coupling of the flavonoid derivatives with the aminoacid residues involved on 1N26 protein surface.

Compounds	Aminoacids Residues
Madindoline A	Lys ₁₀₅ ; Leu ₁₀₈ ; Ser ₁₀₉ ; Asn ₁₁₀ ; Val ₁₁₂ ; Gln ₁₅₈ ; Asn ₂₂₆
Clarithromycin	Leu ₁₀₈ ; Asn ₂₂₆ ; Ser ₂₂₇
Tenidap	Leu ₁₀₈ ; Asn ₂₂₆
1	Leu ₁₀₈ ; Asn ₂₂₆ ; Ser ₂₂₇ ; Phe ₂₂₉
2	Leu ₁₀₈ ; Asn ₂₂₆ ; Ser ₂₂₇ ; Ser ₂₂₈ ; Phe ₂₂₉
3	Leu ₁₀₈ ; Asn ₂₂₆ ; Ser ₂₂₇ ; Ser ₂₂₈ ; Phe ₂₂₉
4	Phe ₁₀₃ ; Lys ₁₀₅ ; Ser ₁₀₆ ; Ser ₁₀₉ ; Val ₁₁₂ ; Asn ₂₂₆
5	Phe ₁₀₃ ; Lys ₁₀₅ ; Ser ₁₀₉ ; Asn ₁₁₀ ; Val ₁₁₂ ; Gln ₁₅₈
6	Arg ₁₀₄ ; Leu ₁₀₈ ; Asn ₁₁₀
7	Leu ₁₀₈ ; Ser ₁₀₉ ; Asn ₁₁₀ ; Asn ₂₂₆ ; Ser ₂₂₇ ; Ser ₂₂₈ ; Phe ₂₂₉
8	Leu ₁₀₈ ; Asn ₂₂₆ ; Ser ₂₂₇ ; Ser ₂₂₈ ; Phe ₂₂₉ ; Met ₉₀₂
9	Leu ₁₀₈ ; Asn ₁₁₀ ; Gln ₁₅₈
10	Leu ₁₀₈ ; Ser ₁₀₉ ; Asn ₂₂₆ ; Ser ₂₂₇ ; Ser ₂₂₈ ; Phe ₂₂₉
11	Ser ₁₀₆ ; Leu ₁₀₈ ; Ser ₁₀₉ ; Asn ₁₁₀ ; Gln ₁₅₈ ; Asn ₂₂₆ ; Ser ₂₂₆ ; Phe ₂₂₉
12	Leu ₁₀₈ ; Ser ₁₀₉ ; Asn ₁₁₀ ; Gln ₁₅₈ ; Asn ₂₂₆ ; Ser ₂₂₇
13	Ser ₁₀₉ ; Asn ₁₁₀ ; Val ₁₁₂ ; Gln ₁₅₈
14	Asp ₂₂₁ ; His ₂₂₃ ; Asn ₂₂₆
15	Leu ₁₀₈ ; Ser ₁₀₉ ; Asn ₁₁₀ ; Gln ₁₅₈ ; Ser ₂₂₇
16	Leu ₁₀₈ ; Ser ₁₀₉ ; Asn ₁₁₀ ; Gln ₁₅₈ ; Asn ₂₂₆ ; Ser ₂₂₇
17	Ser ₁₀₆ ; Leu ₁₀₈ ; Ser ₁₀₉ ; Asn ₁₁₀ ; Gln ₁₅₈ ; Asn ₂₂₆ ; Ser ₂₂₇
18	Ser ₁₀₉ ; Ser ₂₂₄ ; Asn ₂₂₆
19	Leu ₁₀₈ ; Asn ₂₂₆ ; Ser ₂₂₇ ; Ser ₂₂₈ ; Phe ₂₂₉
20	Leu ₁₀₈ ; Ser ₁₀₉ ; Asn ₁₁₀ ; Gln ₁₅₈ ; Asn ₂₂₆ ; Ser ₂₂₇ ; Ser ₂₂₈ ; Phe ₂₂₉

3.3. Bond energies analysis.

Some reports indicate that protein-ligand complex formation can depend on some thermodynamic parameters such as free energy of binding, inhibition constant, van der Waals + hydrogen bond + desolv energy (Vander Walls Forces + Hydrogen bonds + desolv Energy), electrostatic energy, and total intermolecular energy [49, 50]. For this reason, this research aimed to evaluate some theoretical thermodynamic parameters involved in the interaction of flavonoid derivatives (1-20) with 1N26 protein surface using DockingServer software (Table 3).

Table 3. Thermodynamic parameters involved in interacting flavonoid derivatives with 1N26 protein surface using DockingServer software.

Compound	Est: Free Energy of Binding [kcal/mol]	Inhibition Constant, Ki [mM]	Inhibition Constant, Ki [mM]	Electrostatic Energy [kcal/mol]	Total Intermolec. Energy [kcal/mol]	Interact. Surface
Madindoline A	-3.74	1.81	-4.96	-0.02	-4.98	591.806
Clarithromycin	-3.47	2.87	-3.23	+0.01	-3.22	549.693
Tenidap	-4.13	933.64	-4.80	+0.06	-4.75	493.776
1	-3.91	1.36	-3.23	-0.02	-3.25	376.043
2	-4.06	1.05	-2.91	-0.00	-2.91	371.474
3	-2.96	6.71	-3.05	-0.06	-3.11	439.282
4	-2.88	7.75	-3.27	-0.15	-3.42	399.39
5	-3.99	1.18	-3.35	-0.29	-3.65	406.657
6	-4.22	810.71	-4.31	-0.07	-4.37	424.803
7	-4.15	914.07	-4.67	-0.04	-4.72	515.823
8	-3.44	3.01	-4.28	-0.05	-4.33	426.573
9	-4.48	520.61	-3.57	-0.01	-3.58	409.904
10	-3.84	1.52	-4.29	-0.04	-4.32	431.991
11	-3.58	2.39	-3.80	-0.09	-3.89	521.265
12	-4.66	382.15	-3.57	-0.03	-3.61	568.387
13	-3.94	1.30	-3.41	-0.15	-3.55	392.611

Compound	Est: Free Energy of Binding [kcal/mol]	Inhibition Constant, Ki [mM]	Inhibition Constant, Ki [mM]	Electrostatic Energy [kcal/mol]	Total Intermolec. Energy [kcal/mol]	Interact. Surface
14	-4.11	978.16	-3.74	-0.23	-3.97	409.879
15	-4.38	618.24	-4.06	-0.01	-4.07	557.354
16	-4.36	638.30	-3.73	-0.07	-3.80	440.119
17	-5.35	120.74	-3.49	-0.07	-3.56	469.403
18	-4.00	1.17	-1.68	+0.00	-1.67	344.484
19	-3.91	1.36	-3.78	-0.09	-3.87	386.549
20	-4.71	354.08	-4.83	+0.04	-4.79	682.816

The results (Table 3) showed differences in the γ levels for flavonoid derivatives compared with madindoline A, clarithromycin, and tenidap. Besides, the inhibition constant (Ki) for flavonoid derivatives 1, 2, 5, 10, 13, 18, and 19 was lower compared with madindoline A. Other data indicate that Ki for 11 was lower compared with clarithromycin and tenidap. All these data suggest that flavonoid derivatives 1, 2, 5, 10, 11, 13, 18, and 19 could act as interleukin-6 inhibitors, producing changes in the biological activity of interleukin-6; this phenomenon may translated as a decrease in cancer cell growth. However, it is important to mention that the bond length could be a very important factor in the stability of the protein-ligand complex.

3.4. Protein-ligand complex distance.

There are studies to predict the bond distance between different compounds that act as ligands and some biomolecules [51, 52]. Therefore, the protein-ligand formation may be conditioned by the bond length between each atom of flavonoid derivatives with the amino acid residues involved on 1N26 protein surface. For this reason, the bond distance involved in the interaction of flavonoid derivatives 1, 2, 5, 10, 11, 13, 18, 19 with 1N26 protein surface was made taking as a chemical basis the ether group of pyran ring, which is bound to phenyl group involved in the chemical structure of the flavonoid derivatives. The results (Table 4) showed differences in the distance involved on the interaction of flavonoid derivatives with 1N26 protein surface compared with madindoline A, clarithromycin and tenidap. This phenomenon could determine the stability of the protein-ligand complex.

Table 4. Distance of amino acid residues involved in 1N26 protein surface with flavonoid derivatives (1, 2, 5, 10, 11, 13, 18, 19), madindoline A, clarithromycin, and tenidap.

Compound	Aminoacid residues	Distance (Å)
(+)-Madindoline A	Lys ₁₀₅	105.29
	Leu ₁₀₈	106.71
	Asn ₁₁₀	102.90
	Val ₁₁₂	95.12
	Gln ₁₅₈	92.57
	Asn ₂₂₆	110.31
Clarithromycin	Leu ₁₀₈	116.71
	Ser ₁₀₉	105.97
	Ser ₂₂₈	115.99
	Phe ₂₂₉	118.26
Tenidap	Leu ₁₀₈	105.28
	Asn ₂₂₆	109.91
1	Leu ₁₀₈	105.68
	Asn ₂₂₆	109.11
	Ser ₂₂₇	113.03
	Phe ₂₂₉	114.95
2	Leu ₁₀₈	105.69
	Asn ₂₂₆	109.11
	Ser ₂₂₇	113.03
	Ser ₂₂₈	114.80

Compound	Aminoacid residues	Distance (Å)
3	Phe ₂₂₉	114.95
	Phe ₁₀₃	95.35
	Lys ₁₀₅	101.33
	Ser ₁₀₆	104.26
	Val ₁₁₂	96.49
4	Asn ₂₂₆	109.11
	Asp ₂₂₁	109.60
	His ₂₂₃	107.52
	Trp ₂₂₅	106.12
5	Asn ₂₂₆	107.08
	Phe ₁₀₃	95.52
	Lys ₁₀₅	100.62
	Ser ₁₀₉	102.97
	Asn ₁₁₀	100.54
8	Val ₁₁₂	93.19
	Gln ₁₅₈	95.44
	Leu ₁₀₈	104.21
	Asn ₂₂₆	107.67
10	Ser ₂₂₇	111.02
	Phe ₂₂₉	112.68
	Leu ₁₀₈	104.88
	Ser ₁₀₉	101.64
	Asn ₂₂₆	107.61
11	Ser ₂₂₇	111.57
	Ser ₂₂₈	113.48
	Phe ₂₂₉	111.55
	Ser ₁₀₆	104.20
	Leu ₁₀₈	105.60
	Ser ₁₀₉	104.07
	Asn ₁₁₀	101.70
13	Gln ₁₅₀	94.24
	Asn ₂₂₆	108.92
	Ser ₂₂₇	112.94
	Phe ₂₂₉	113.01
18	Ser ₁₀₉	101.66
	Asn ₁₁₀	100.51
	Val ₁₁₂	92.76
	Gln ₁₅₈	95.41
19	Ser ₁₀₉	105.36
	Ser ₂₂₄	107.95
	Asn ₂₂₆	107.77
19	Leu ₁₀₈	104.38
	Asn ₂₂₆	107.12
	Ser ₂₂₇	111.80
	Ser ₂₂₈	113.72
	Phe ₂₂₉	113.45

3.7. Pharmacokinetic evaluation.

In the literature, there are methods to predict several pharmacokinetic parameters [53-55]. For this reason, this study determined different pharmacokinetic parameters for flavonoid derivatives (1, 2, 5, 10, 11, 13, 18, 19) using the SwissADME software (Tables 4 and 5). Results indicate differences in gastrointestinal absorption and metabolism (involving several cytochrome P450 systems) compared with madindoline A, clarithromycin, and tenidap. This could be due to differences in the chemical structure of each flavonoid derivative and their degree of lipophilicity (LogP, see Table 1).

Table 4. Theoretical Pharmacokinetic parameters involved in flavonoid derivatives 1, 2, 5, madindoline A (I), clarithromycin (II), and tenidap (III).

Parameter	Madindoline A	Clarithromycin	Tenidap	1	2	5
GI absorption	High	Low	High	Low	Low	High
BBB permeant	Yes	No	No	No	No	No
P-gp substrate	Yes	Yes	No	No	No	No
CYP1A2 inhibitor	No	No	Yes	No	No	Yes

Parameter	Madindoline A	Clarithromycin	Tenidap	1	2	5
CYP2C19 inhibitor	No	No	Yes	No	No	No
CYP2C9 inhibitor	No	No	Yes	No	No	No
CYP2D6 inhibitor	Yes	No	No	No	No	Yes
CYP3A4 inhibitor	Yes	No	No	No	No	Yes

GI = Gastrointestinal; BBB = Blood-Brain-Barrier; P-gP = P-Glycoprotein; CYP = cytochrome P450 systems

Table 5. Theoretical Pharmacokinetic parameters involved in flavonoid derivatives 10, 11, 13, 18 and 19.

Parameter	10	11	13	18	19
GI absorption	High	Low	High	Low	High
BBB permeant	No	No	No	No	No
P-gp substrate	No	No	No	Yes	No
CYP1A2 inhibitor	Yes	No	Yes	No	Yes
CYP2C19 inhibitor	No	No	No	No	No
CYP2C9 inhibitor	No	No	No	No	No
CYP2D6 inhibitor	Yes	No	Yes	No	Yes
CYP3A4 inhibitor	Yes	No	Yes	No	Yes

3.8. Theoretical toxicity analysis.

Several methods for predicting toxicity degree have been used, such as ProTox-II [56], STopTox [57], ToxAlert [58], q-Tox [59], and others. Analyzing these data, this study determined the possible theoretical toxicity produced by flavonoid derivatives 1, 2, 5, 10, 11, 13, 18, and 19 using the GUSAR software [44]. The results (Table 6) suggest that the compounds madindoline A, clarithromycin, and tenidap require low doses via either intravenous or subcutaneous routes to produce toxicity compared to flavonoid derivatives. These results could be due to the different functional groups involved in each compound.

Table 6. Theoretical toxicity analysis produced by madindoline, clarithromycin, tenidap, and flavonoid derivatives (1, 2, 5, 10, 11, 13, 18, 19).

Compound	Rat IP LD50 [mg/kg]	Rat IV LD50 [mg/kg]	Rat Oral LD50 [mg/kg]	Rat SC LD50 [mg/kg]
Madindoline A	227.90	25.01	896.50	181.30
Clarithromycin	112.80	49.28	2120.00	1627.00
Tenidap	1629.00	151.80	1576.00	1107.00
1	1083.00	801.50	1573.00	622.80
2	1114.00	647.60	2933.00	570.70
5	855.20	185.10	1324.00	3502.00
10	1196.00	297.10	1749.00	2886.00
11	647.20	1832.00	3655.00	4621.00
13	1573.00	372.00	1684.00	2723.00
18	122.00	2132.00	29.53.00	1653.00
19	798.10	200.60	1577.00	2818.00

IP - Intraperitoneal route of administration; IV - Intravenous route of administration; Oral - Oral route of administration; SC - Subcutaneous route of administration

4. Conclusions

The theoretical interaction of flavonoid derivatives (1, 2, 5, 10, 11, 13, 18, 19) with interleukin-6 was determined using DockingServer software. The results showed that flavonoid derivatives 1, 2, 5, 10, 11, 13, 18, and 19 could act as interleukin-6 inhibitors, producing changes in the biological activity interleukin-6. In conclusion, these flavonoid derivatives could be a good alternative as interleukin-6 inhibitors to decrease cancer cell growth.

Funding

This research received no external funding.

Acknowledgments

None.

Conflicts of Interest

We declare that this manuscript has no conflict of financial interests (political, personal, religious, ideological, academic, intellectual, commercial, or otherwise) for publication.

References

1. O'Sullivan, D.E.; Sutherland, R.L.; Town, S.; Chow, K.; Fan, J.; Forbes, N.; Heitman, S.J.; Hilsden, R.J.; Brenner, D.R. Risk Factors for Early-Onset Colorectal Cancer: A Systematic Review and Meta-analysis. *Clin Gastroenterol Hepatol* **2022**, *20*, 1229-1240, <https://doi.org/10.1016/j.cgh.2021.01.037>.
2. Xia, C.; Dong, X.; Li, H.; Cao, M.; Sun, D.; He, S.; Yang, F.; Yan, X.; Zhang, S.; Li, N.; Chen, W. Cancer statistics in China and United States, 2022: profiles, trends, and determinants. *Chin Med J* **2022**, *135*, 584-590, <http://doi.org/10.1097/CM9.0000000000002108>.
3. Hanahan, D. Hallmarks of Cancer: New Dimensions. *Cancer Discov* **2022**, *12*, 31-46, <https://doi.org/10.1158/2159-8290.CD-21-1059>.
4. Chandrashekar, D.S.; Karthikeyan, S.K.; Korla, P.K.; Patel, H.; Shovon, A.R.; Athar, M.; Netto, G.J.; Qui, Z.S.; Kumar, S.; Manne, U.; Creighton, C.J.; Varambally, S. UALCAN: An update to the integrated cancer data analysis platform. *Neoplasia* **2022**, *25*, 18-27, <https://doi.org/10.1016/j.neo.2022.01.001>.
5. Dharwadkar, P.; Greenan, G.; Stoffel, E.M.; Burstein, E.; Pirzadeh-Miller, S.; Lahiri, S.; Mauer, C.; Singal, A.G.; Murphy, C.C. Racial and Ethnic Disparities in Germline Genetic Testing of Patients With Young-Onset Colorectal Cancer. *Clin Gastroenterol Hepatol* **2022**, *20*, 353-361, <https://doi.org/10.1016/j.cgh.2020.12.025>.
6. Jiang, Y.; Meyers, T.J.; Emeka, A.A.; Cooley, L.F.; Cooper, P.R.; Lancki, N.; Helenowski, I.; Kachuri, L.; Lin, D.W.; Stanford, J.L.; Newcomb, L.F.; Kolb, S.; Finelli, A.; Fleshner, N.E.; Komisarenko, M.; Eastham, J.A.; Ehdaie, B.; Benfante, N.; Logothetis, C.J.; Gregg, J.R.; Perez, C.A.; Garza, S.; Kim, J.; Marks, L.S.; Delfin, M.; Barsa, D.; Vesprini, D.; Klotz, L.H.; Loblaw, A.; Mamedov, A.; Goldenberg, S.L.; Higano, C.S.; Spillane, M.; Wu, E.; Carter, H.B.; Pavlovich, C.P.; Mamawala, M.; Landis, T.; Carroll, P.R.; Chan, J.M.; Cooperberg, M.R.; Cowan, J.E.; Morgan, T.M.; Siddiqui, J.; Martin, R.; Klein, E.A.; Brittain, K.; Gotwald, P.; Barocas, D.A.; Dallmer, J.R.; Gordetsky, J.B.; Steele, P.; Kundu, S.D.; Stockdale, J.; Roobol, M.J.; Venderbos, L.D.F.; Sanda, M.G.; Arnold, R.; Patil, D.; Evans, C.P.; Dall'Era, M.A.; Vij, A.; Costello, A.J.; Chow, K.; Corcoran, N.M.; Rais-Bahrami, S.; Phares, C.; Scherr, D.S.; Flynn, T.; Karnes, R.J.; Koch, M.; Dhondt, C.R.; Nelson, J.B.; McBride, D.; Cookson, M.S.; Stratton, K.L.; Farriester, S.; Hemken, E.; Stadler, W.M.; Pera, T.; Banionyte, D.; Bianco, F.J. Jr; Lopez, I.H.; Loeb, S.; Taneja, S.S.; Byrne, N.; Amling, C.L.; Martinez, A.; Boileau, L.; Gaylis, F.D.; Petkewicz, J.; Kirwen, N.; Helfand, B.T.; Xu, J.; Scholtens, D.M.; Catalona, W.J.; Witte, J.S. Genetic factors associated with prostate cancer conversion from active surveillance to treatment. *HGG Adv* **2022**, *3*, 100070, <https://doi.org/10.1016/j.xhgg.2021.100070>.
7. Reece, A.S.; Hulse, G.K. Geospatiotemporal and causal inference study of cannabis and other drugs as risk factors for female breast cancer USA 2003–2017. *Environ Epigenetics* **2022**, *8*, dvac006, <https://doi.org/10.1093/eep/dvac006>.
8. Rahman, T.; Sahrman, J.M.; Olsen, M.A.; Nickel, K.B.; Miller, J.P.; Ma, C.; Grucza, R.A. Risk of Breast Cancer With Prolactin Elevating Antipsychotic Drugs: An Observational Study of US Women (Ages 18–64 Years). *J Clin Psychopharmacol* **2022**, *42*, 7-16, <https://doi.org/10.1097/JCP.0000000000001513>.
9. Fan, Y.; Qiu, Y.; Wang, J.; Chen, Q.; Wang, S.; Wang, Y.; Li, Y.; Weng, Y.; Qian, J.; Chen, F.; Wang, J.; Shi, B.; Pan, L.; Lin, L.; Lin, L.; He, B.; Liu, F.; Association Between Dietary Fatty Acid Pattern and Risk of Oral Cancer. *Front Nutr* **2022**, *9*, <https://doi.org/10.3389/fnut.2022.864098>.
10. Phua, Z.J.; MacInnis, R.J.; Jayasekara, H. Cigarette smoking and risk of second primary cancer: a systematic review and meta-analysis. *Cancer Epidemiol* **2022**, *78*, 102160, <https://doi.org/10.1016/j.canep.2022.102160>.
11. Kwan, E.M.; Spain, L.; Anton, A.; Gan, C.L.; Garrett, L.; Chang, D.; Liow, E.; Bennett, C.; Zheng, T.; Yu, J.; Dai, C.; Du, P.; Jia, S.; Fettke, H.; Abou-Seif, C.; Kothari, G.; Shaw, M.; Parente, P.; Pezaro, C.; Tran, B.; Siva, S.; Azad, A.A. Avelumab Combined with Stereotactic Ablative Body Radiotherapy in Metastatic Castration-resistant Prostate Cancer: The Phase 2 ICE-PAC Clinical Trial. *Eur Urol* **2022**, *81*, 253-262, <https://doi.org/10.1016/j.eururo.2021.08.011>.

12. Al-Tarawneh, S.F.; Dahmash, E.Z.; Alyami, H.; Abu-Doleh, S.M.; Al-Ali, S.; Iyire, A.; Abuthawabeh, R. Mechanistic modelling of targeted pulmonary delivery of dactinomycin iron oxide-loaded nanoparticles for lung cancer therapy. *Pharm Dev Technol* **2022**, *27*, 1057-1068, <http://doi.org/10.1080/10837450.2022.2152047>.
13. Bradley, R.; Braybrooke, J.; Gray, R.; Hills, R.K.; Liu, Z.; Pan, H.; Peto, R.; Dodwell, D.; McGale, P.; Taylor, C.; Francis, P.A.; Gnant, M.; Perrone, F.; Regan, M.M.; Berry, R.; Boddington, C.; Clarke, M.; Davies, C.; Davies, L.; Duane, F.; Evans, V.; Gay, J.; Gettins, L.; Godwin, J.; James, S.; Liu, H.; MacKinnon, E.; Mannu, G.; McHugh, T.; Morris, P.; Read, S.; Straiton, E.; Jakesz, r.; Fesl, C.; Pagani, O.; Gelber, R.; De Laurentiis, M.; De Placido, S.; Gallo, C.; Albain, K.; Anderson, S.; Arriagada, R.; Bartlett, J.; Bergsten-Nordström, E.; Bliss, J.; Brain, E.; Carey, L.; Coleman, R.; Cuzick, J.; Davidson, N.; Del Mastro, L.; Di Leo, A.; Dignam, J.; Dowsett, M.; Ejlertsen, B.; Goetz, M.; Goodwin, P.; Halpin-Murphy, P.; Hayes, D.; Hill, C.; Jagsi, R.; Janni, W.; Loibl, S.; Mamounas, E.P.; Martin, M.; Mukai, H.; Nekljudova, V.; Norton, L.; Ohashi, Y.; Pierce, L.; Poortmans, P.; Pritchard, K.I.; Raina, V.; Rea, D.; Robertson, J.; Rutgers, E.; Spanic, T.; Sparano, J.; Steger, G.; Tang, G.; Toi, M.; Tutt, A.; Viale, G.; Wang, X.; Whelan, T.; Wilcken, N.; Wolmark, N.; Cameron, D.; Bergh, J. Swain, S.M. Aromatase inhibitors versus tamoxifen in premenopausal women with oestrogen receptor-positive early-stage breast cancer treated with ovarian suppression: a patient-level meta-analysis of 7030 women from four randomised trials. *Lancet Oncol* **2022**, *23*, 382-392, [https://doi.org/10.1016/S1470-2045\(21\)00758-0](https://doi.org/10.1016/S1470-2045(21)00758-0).
14. Cheng, A.L.; Qin, S.; Ikeda, M.; Galle, P.R.; Ducreux, M.; Kim, T.Y.; Lim, H.Y.; Kudo, M.; Breder, V.; Merle, P.; Kaseb, A.O.; Li, D.; Verret, W.; Ma, N.; Nicholas, A.; Wnag, Y.; Li, L.; Zhu, A.X.; Finn, R.S. Updated efficacy and safety data from IMbrave150: Atezolizumab plus bevacizumab vs. sorafenib for unresectable hepatocellular carcinoma. *J Hepatol* **2022**, *76*, 862-873, <https://doi.org/10.1016/j.jhep.2021.11.030>.
15. Li, Y.; Ma, J.; Qin, X.H.; Hu, C.Y. The efficacy and safety of dutasteride and finasteride in patients with benign prostatic hyperplasia: a systematic review and meta-analysis. *Transl Androl Urol* **2022**, *11*, 313-324, <https://doi.org/10.21037/tau-22-58>.
16. Schoot, R.A.; Otth, M.A.; Frederix, G.W.J.; Leufkens, H.G.M.; Vassal, G. Market access to new anticancer medicines for children and adolescents with cancer in Europe. *Eur J Cancer* **2022**, *165*, 146-153, <https://doi.org/10.1016/j.ejca.2022.01.034>.
17. Ashrafizadeh, M.; Saebfar, H.; Gholami, M.H.; Hushmandi, K.; Zabolian, A.; Bikarannejad, P.; Hashemi, M.; Daneshi, S.; Mirzaei, S.; Sharifi, E.; Kumar, A.P.; Khan, H.; Hossein, H.H.S.; Vosough, M.; Rabiee, N.; Thakur, V.K.; Makvandi, P.; Mishra, Y.K.; Tay, F.R.; Wang, Y.; Zarrabi, A.; Orive, G.; Mostafavi, E. Doxorubicin-loaded graphene oxide nanocomposites in cancer medicine: Stimuli-responsive carriers, co-delivery and suppressing resistance. *Expert Opin Drug Deliv* **2022**, *19*, 355-382, <https://doi.org/10.1080/17425247.2022.2041598>.
18. Lee, K.J.; Chow, V.; Weissman, A.; Tulpule, S.; Aldoss, I.; Akhtari, M. Clinical use of blinatumomab for B-cell acute lymphoblastic leukemia in adults. *Ther Clin Risk Manag* **2016**, *12*, 1301-1310, <https://doi.org/10.2147/TCRM.S84261>.
19. Merz, B.; Hager, T. Defusing adverse effects of anticancer drugs. *JAMA* **1983**, *250*, 459, <http://doi.org/doi:10.1001/jama.1983.03340040011008>.
20. Nayfield, S.G.; Gorin, M.B. Tamoxifen-associated eye disease. A review. *J Clin Oncol* **1996**, *14*, 1018-1026, <https://doi.org/10.1200/jco.1996.14.3.1018>.
21. Sinaga, S.P.; Lumbangaol, D.A.; Iksen, I.; Situmorand, R.; Gurning, K. DETERMINATION OF PHENOLIC, FLAVONOID CONTENT, ANTIOXIDANT AND ANTIBACTERIAL ACTIVITIES OF SERI (Muntingia calabura L.) LEAVES ETHANOL EXTRACT FROM NORTH SUMATERA, INDONESIA. *Rasayan J Chem* **2022**, *15*, 1534-1538, <http://doi.org/10.31788/RJC.2022.1526730>.
22. Wang, Y.; Liu, X.J.; Chen, J.B.; Cao, J.P.; Li, X.; Sun, C.D. Citrus flavonoids and their antioxidant evaluation. *Crit Rev Food Sci Nutr* **2022**, *62*, 3833-3854, <https://doi.org/10.1080/10408398.2020.1870035>.
23. Liu, Z.; Zhao, M.; Wang, X.; Li, C.; Wang, J.; Liu, Z.; Shen, X.; Zhou, D. Response surface methodology-optimized extraction of flavonoids with antioxidant and antimicrobial activities from the exocarp of three genera of coconut and characterization by HPLC-IT-TOF-MS/MS. *Food Chem* **2022**, *391*, 132966, <https://doi.org/10.1016/j.foodchem.2022.132966>.
24. Al-Khayri, J.M.; Sahana, G.R.; Nagella, P.; Joseph, B.V.; Alessa, F.M.; Al-Mssallem, M.Q. Flavonoids as Potential Anti-Inflammatory Molecules: A Review. *Molecules* **2022**, *27*, 2901, <https://doi.org/10.3390/molecules27092901>.

25. Yang, T.; Hu, Y.; Yan, Y.; Zhou, W.; Chen, G.; Zeng, X.; Cao, Y. Characterization and Evaluation of Antioxidant and Anti-Inflammatory Activities of Flavonoids from the Fruits of *Lycium barbarum*. *Foods* **2022**, *11*, 306, <https://doi.org/10.3390/foods11030306>.
26. Felice, M.R.; Maugeri, A.; De-Sarro, G.; Navarra, M.; Barreca, D. Molecular Pathways Involved in the Anti-Cancer Activity of Flavonols: A Focus on Myricetin and Kaempferol. *Int J Mol Sci* **2022**, *23*, 4411, <https://doi.org/10.3390/ijms23084411>.
27. Gu, Y.; Zheng, Q.; Fan, G.; Liu, R. Advances in Anti-Cancer Activities of Flavonoids in *Scutellariae radix*: Perspectives on Mechanism. *Int J Mol Sci* **2022**, *23*, 11042, <https://doi.org/10.3390/ijms231911042>.
28. Maleki, N.; Yavari, N.; Ebrahimi, M.; Faiz, A.F.; Ravesh, R.K.; Sharbati, A.; Panji, M.; Lorian, K.; Gravand, A.; Abbasi, M.; Abazari, O.; Mehr, M.S.; Eskandari, Y. Silibinin exerts anti-cancer activity on human ovarian cancer cells by increasing apoptosis and inhibiting epithelial-mesenchymal transition (EMT). *Gene* **2022**, *823*, 146275, <https://doi.org/10.1016/j.gene.2022.146275>.
29. Li, T.; Li, Y. Quercetin acts as a novel anti-cancer drug to suppress cancer aggressiveness and cisplatin-resistance in nasopharyngeal carcinoma (NPC) through regulating the Yes-associated protein/Hippo signaling pathway. *Immunobiol* **2022**, *228*, 152324, <https://doi.org/10.1016/j.imbio.2022.152324>.
30. Geng, A.; Xu, S.; Yao, Y.; Qian, Z.; Wang, X.; Sun, J.; Zhang, J.; Shi, F.; Chen, Z.; Zhang, W.; Mao, Z.; Lu, W.; Jiang, Y. Chrysin impairs genomic stability by suppressing DNA double-strand break repair in breast cancer cells. *Cell Cycle* **2022**, *21*, 379-391, <https://doi.org/10.1080/15384101.2021.2020434>.
31. Shafiee, G.; Saidijam, M.; Tayebinia, H.; Khodadadi, I. Beneficial effects of genistein in suppression of proliferation, inhibition of metastasis, and induction of apoptosis in PC3 prostate cancer cells. *Arch Physiol Biochem* **2022**, *128*, 694-702, <https://doi.org/10.1080/13813455.2020.1717541>.
32. Zhang, S.Y.; Lu, Y.Y.; He, X.L.; Su, Y.; Hu, F.; Wei, X.S.; Pan, M.J.; Zhou, Q.; Yang, W.B. Lutein inhibits tumor progression through the ATR/Chk1/p53 signaling pathway in non-small cell lung cancer. *Phytother Res* **2022**, *37*, 1260-1273, <https://doi.org/10.1002/ptr.7682>.
33. Yousuf, M.; Shamsi, A.; Khan, S.; Khan, P.; Shahwan, M.; Elaslali, A.M.; Haque, Q.M.R.; Hassan, M.I. Naringenin as a potential inhibitor of human cyclin-dependent kinase 6: Molecular and structural insights into anti-cancer therapeutics. *Int J Biol Macromol* **2022**, *213*, 944-954, <https://doi.org/10.1016/j.ijbiomac.2022.06.013>.
34. Dukel, M. Combination of naringenin and epicatechin sensitizes colon carcinoma cells to anoikis via regulation of the epithelial-mesenchymal transition (EMT). *Mol Cell Toxicol* **2023**, *19*, 187-203, <http://doi.org/10.1007/s13273-022-00317-y>.
35. Camargo, C.A.; Gomes-Marcondes, M.C.C.; Wutzki, N.C.; Aoyama, H. Naringin inhibits tumor growth and reduces interleukin-6 and tumor necrosis factor α levels in rats with Walker 256 carcinosarcoma. *Anticancer Res* **2012**, *32*, 129-133.
36. Figueroa-Valverde, L.; Díaz-Cedillo, F.; Rosas-Nexticapa, M.; Virginia, M.; Armad, M.; Lopez-Ramos, M.; Lopez-Gutierrez, T.; Alvarez-Ramirez, M.; Cervantes-Ortega, C.; Cauich-Carrillo, R. Design and Synthesis of Two Azete Derivatives Using some Chemical Strategies. *Biointerface Res Appl Chem* **2022**, *12*, 5567-5578, <https://doi.org/10.33263/BRIAC124.55675578>.
37. Varghese J.N.; Moritz R.L.; Lou M.Z.; van Donkelaar, A.; Ji H.; Ivancic N.; Branson, K.M.; Hall, N.E.; Simpson R.J. Structure of the extracellular domains of the human interleukin-6 receptor α -chain. *Proc Natl Acad Sci* **2002**, *99*, 15959-15964, <http://doi.org/10.1073/pnas.232432399>.
38. Sabui S.; Subramanian V.S.; Ghosal A.; Kapadia R.; Said H. Structure-Function relationship of the human mitochondrial thiamin pyrophosphate transporter (MTPPT; SLC25A19): Critical roles for Ser34, Lys 291 and His137. *The FASEB Journal* **2016**, *30*, 973-2. https://doi.org/10.1096/fasebj.30.1_supplement.973.2
39. Oliveira, F.A.; Pinto, A.C.S.; Duarte, C.L.; Taranto, A.G.; Lorenzato-Junior, E., Cordeiro, C.F.; Carvalho, D.T.; Varotti, F.P.; Fonseca, A.L. Evaluation of antiplasmodial activity in silico and in vitro of N-acylhydrazone derivatives. *BMC Chem* **2022**, *16*, <https://doi.org/10.1186/s13065-022-00843-9>.
40. Ullah, H.; Khan, A.; Bibi, T.; Ahmad, S.; Shehzad, O., Ali, H.; Seo, E.K.; Khan, S. Comprehensive in vivo and in silico approaches to explore the hepatoprotective activity of poncirin against paracetamol toxicity. *Naunyn-Schmiedeberg's Arch Pharmacol* **2022**, *395*, 195-215, <https://doi.org/10.1007/s00210-021-02192-1>.
41. Da-Rocha, M.N.; Marinho, E.S.; Marinho, M.M.; dos Santos, H.S. Virtual Screening in Pharmacokinetics, Bioactivity, and Toxicity of the *Amburana cearensis* Secondary Metabolites. *Biointerface Res Appl Chem* **2022**, *12*, 8471-8491, <https://doi.org/10.33263/BRIAC126.84718491>.

42. Goreci, C.Y. Synthesis and comparative spectroscopic studies, HOMO–LUMO analysis and molecular docking studies of 3,3'-(1,4-phenylene)bis[2-(6-chloropyridin-3-yl)prop-2-enitrile] based on DFT. *J Mol Struct* **2022**, *1263*, 133149, <https://doi.org/10.1016/j.molstruc.2022.133149>.
43. Manoj, K.P.; Elangovan, N.; Chandrasekar, S. Synthesis, XRD, Hirshfeld surface analysis, ESP, HOMO–LUMO, quantum chemical modeling and anticancer activity of di(*p*-methyl benzyl)(dibromo)(1,10-phenanthroline) tin (IV) complex. *Inorg Chem Commun* **2022**, *139*, 109324, <https://doi.org/10.1016/j.inoche.2022.109324>.
44. Antonczak, S. Electronic description of four flavonoids revisited by DFT method. *J Mol Struct: THEOCHEM* **2008**, *856*, 38–45, <https://doi.org/10.1016/j.theochem.2008.01.014>.
45. Eugène, E.A.; Robert, N.B.; Ganiyou, A.; Denis, Y.K.; Ané, A.; Sawaliho, B.E.H. Catechin and Epicatechin. What's the More Reactive?. *Compt Chem* **2022**, *10*, 53–70, <https://doi.org/10.4236/cc.2022.102003>.
46. Sunazuka, T.; Hirose, T.; Shirahata, T.; Harigaya, Y.; Hayashi, M.; Komiyama, K.; Ōmura, S.; Smith, A.B. Total Synthesis of (+)-Madindoline A and (–)-Madindoline B, Potent, Selective Inhibitors of Interleukin 6. Determination of the Relative and Absolute Configurations. *J Am Chem Soc* **2000**, *122*, 2122–2123, <https://doi.org/10.1021/ja9938074>.
47. Sassa, K.; Mizushima, Y.; Kobayashi, M. Differential Modulatory Effects of Clarithromycin on the Production of Cytokines by a Tumor. *Antimicrob Agents Chemother* **1999**, *43*, 2787–2789, <https://doi.org/10.1128/AAC.43.11.2787>.
48. Kaur, S.; Bansal, Y. Design, molecular Docking, synthesis and evaluation of xanthoxylin hybrids as dual inhibitors of IL-6 and acetylcholinesterase for Alzheimer's disease. *Bioorg Chem* **2022**, *121*, 105670, <https://doi.org/10.1016/j.bioorg.2022.105670>.
49. Figueroa-Valverde, L.; Rosas-Nexticapa, M.; Montserrat, M.G.; Díaz-Cedillo, F.; López-Ramos, M.; Alvarez-Ramirez, M.; Mateu-Armad, M.V.; Gutierrez, T.L. Synthesis and Theoretical Interaction of 3-(2-oxabicyclo [7.4.0]trideca-1(13),9,11-trien-7-yn-12-yloxy)-steroid Derivative with 17β-hydroxysteroid Dehydrogenase Enzyme Surface. *Biointerface Res Appl Chem* **2022**, *13*, 266, <https://doi.org/10.33263/BRIAC133.266>.
50. Ulhas, R.S.; Malaviya, A. In-silico validation of novel therapeutic activities of withaferin a using molecular docking and dynamics studies. *J Biomolec Struct Dyn* **2022**, *41*, 5045–5056, <https://doi.org/10.1080/07391102.2022.2078410>.
51. Angles, R.; Arenas-Salinas, M.; García, R.; Reyes, J.; Pohl, E. GSP4PDB: a web tool to visualize, search and explore protein-ligand structural patterns. *BMC Bioinform* **2020**, *21*, <https://doi.org/10.1186/s12859-020-3352-x>.
52. Shen, C.; Zhang, X.; Deng, Y.; Gao, J.; Wang, D.; Xu, L.; Pan, P.; Hou, T.; Kang, Y. Boosting Protein-Ligand Binding Pose Prediction and Virtual Screening Based on Residue–Atom Distance Likelihood Potential and Graph Transformer. *J Med Chem* **2022**, *65*, 10691–10706, <https://doi.org/10.1021/acs.jmedchem.2c00991>.
53. Mekky, A. E.M.; Sanad, S.M.H.; Abdelfattah, A.M. Tandem synthesis, antibacterial evaluation and SwissADME prediction study of new bis (1,3,4-oxadiazoles) linked to arene units. *Mendeleev Commun* **2022**, *32*, 612–614, <https://doi.org/10.1016/j.mencom.2022.09.014>.
54. Ahmed, A.A.M.; Mekky, A.E.M.; Sanad, S.M.H. New bis (pyrazolo[3,4-*b*]pyridines) and bis(thieno[2, 3-*b*]pyridines) as potential acetylcholinesterase inhibitors: synthesis, in vitro and SwissADME prediction study. *J Iran Chem Soc* **2022**, *19*, 4457–4471, <https://doi.org/10.1007/s13738-022-02614-8>.
55. Al-Azzam, K.M.; Negim, E.S.; Aboul-Enein, H.Y. ADME studies of TUG-770 (a GPR-40 inhibitor agonist) for the treatment of type 2 diabetes using SwissADME predictor: In silico study. *J Appl Pharm Sci* **2022**, *12*, <http://doi.org/10.7324/JAPS.2022.120418>.
56. Banerjee, P.; Ulker, O.C. Combinative *ex vivo* studies and *in silico* models ProTox-II for investigating the toxicity of chemicals used mainly in cosmetic products. *Toxicol Mech Methods* **2022**, *32*, 542–548, <https://doi.org/10.1080/15376516.2022.2053623>.
57. Chikowe, I.; Phiri, A.C.; Mbewe, K.P.; Matekenya, D. In-silico evaluation of Malawi essential medicines and reactive metabolites for potential drug-induced toxicities. *BMC Pharmacol Toxicol* **2021**, *22*, <https://doi.org/10.1186/s40360-021-00499-6>.
58. Dos-Santos, L.F.; Defrenne, L.; Krebs-Brown, A. Comparison of three microbial assay procedures for measuring toxicity of chemical compounds: ToxAlert® 10, CellSense and Biolog MT2 microplates. *Anal Chim Acta* **2002**, *456*, 41–54, [https://doi.org/10.1016/S0003-2670\(01\)00907-2](https://doi.org/10.1016/S0003-2670(01)00907-2).
59. Moorthy, N.S.H.N.; Vittal, U.B.; Karthikeyan, C.; Thangapandian, V.; Venkadachallam, A.P.; Trivedi, P. Synthesis, antifungal evaluation and *in silico* study of novel Schiff bases derived from 4-amino-5(3,5-

dimethoxy-phenyl)-4*H*-1,2,4-triazol-3-thiol. *Arab J Chem* **2017**, *10*, S3239-S3244,
<https://doi.org/10.1016/j.arabjc.2013.12.021>.